UNIVERSITY OF BIRMINGHAM

Physics potential of CLIC operation at 380 GeV

Alasdair Winter

Moriond QCD 2017

On Behalf of the CLICdp Collaboration

Overview

- What is the CLIC experiment?
  - Accelerator design
  - Energy staging
  - Detector concepts
- Higgs Physics
  - "The golden production mode"
  - Model independent total width
  - Higgs couplings
  - Mass determination
- Top Physics
  - Mass measurement
  - Electroweak couplings
  - Rare decays

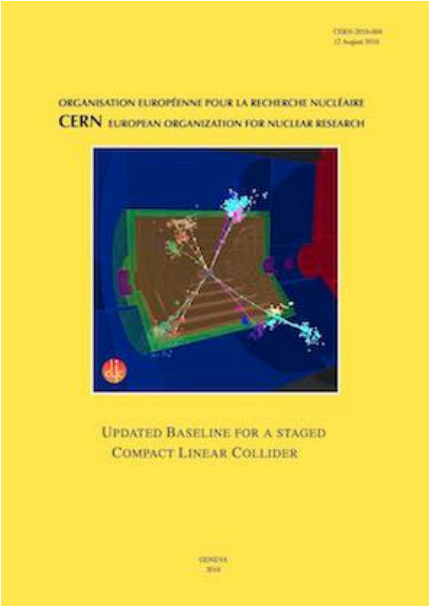

CLIC Rebaseline Document

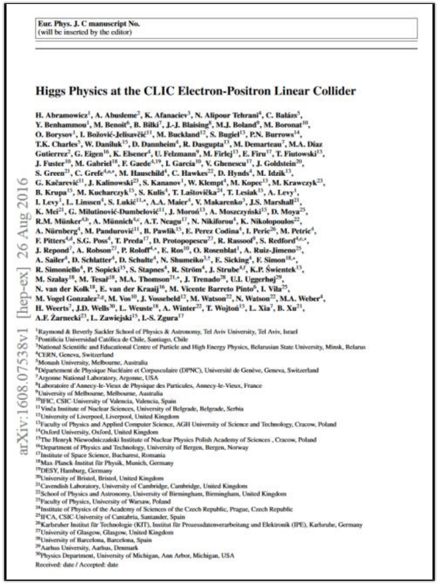

Eur. Phys. J. C manuscript No.
(will be inserted by the editor)

Higgs Physics at the CLIC Electron-Positron Linear Collider

arXiv:1608.07538v1 [hep-ex] 26 Aug 2016

Higgs Summary Paper

CLIC - Compact Linear Collider

- Multi-TeV e^+e^- collider
- $350\text{GeV} < \sqrt{s} < 3\text{TeV}$
- $P(e^-) = \pm 80\%$
- Two beam acceleration
  - Up to $100\,\text{MV/m}$
- $L \sim 1.5 \times 10^{34}\,\text{cm}^{-2}\text{s}^{-1}$
- 11km Tunnel
- Cost: 6.7BCHF
- Power:250MW

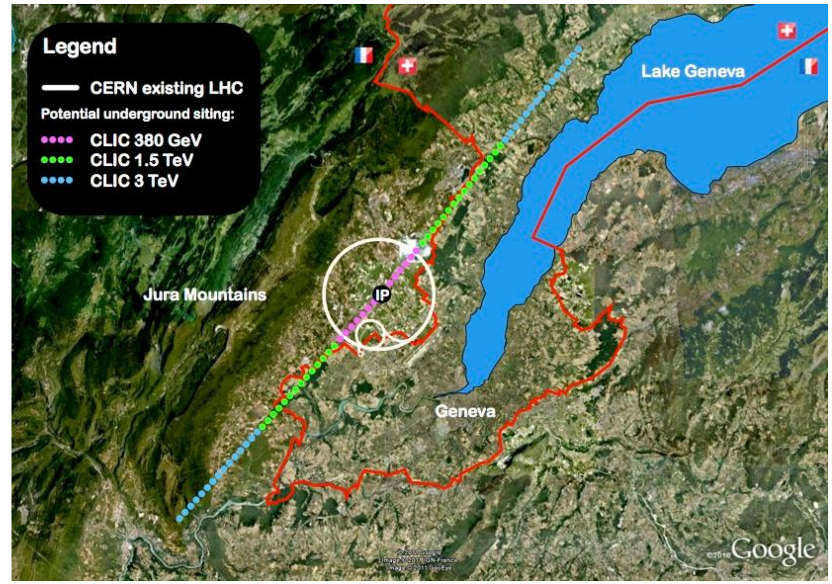

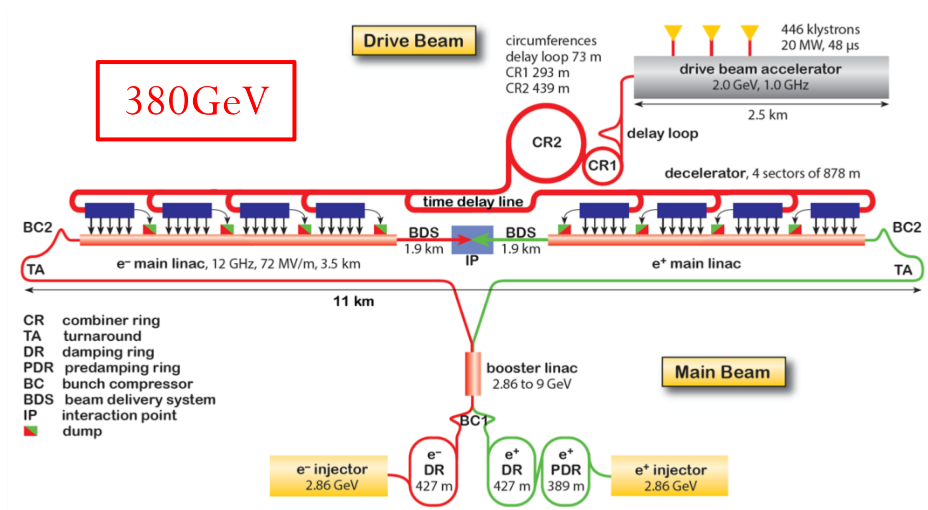

Energy Staging

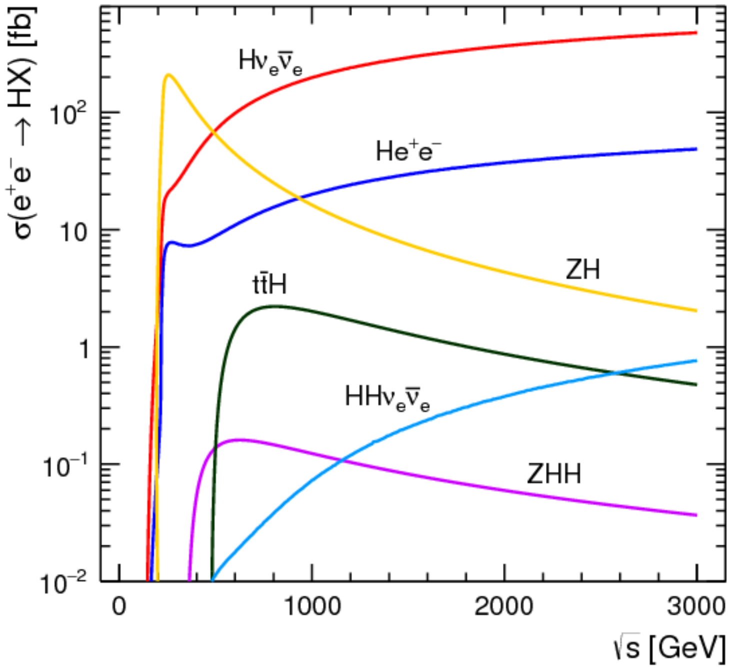

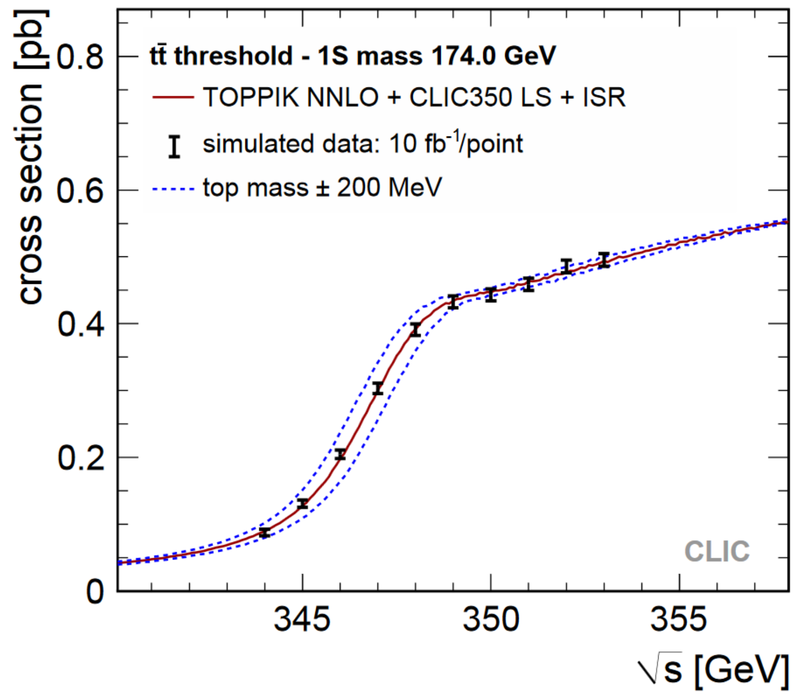

Stage	$\sqrt{s}$ (GeV)	Integrated Luminosity (fb^{-1})
1	380	500
-	350	100
2	1500	1500
3	3000	3000

Right: K.Seidel et al., Eur. Phys. J. C73 (2013) 2530

Detector

- New CLIC detector design developed
- Based on the detector concepts designed for ILC- ILD and SiD
- Studies performed using full GEANT4 simulations
- Optimised for particle flow based approach
- Excellent jet energy resolution (σ_E / E~3.5%) essential for separation of W/Z jets

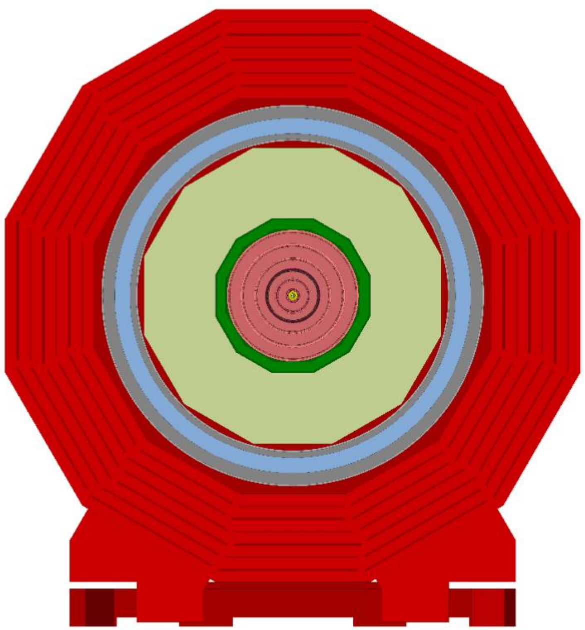

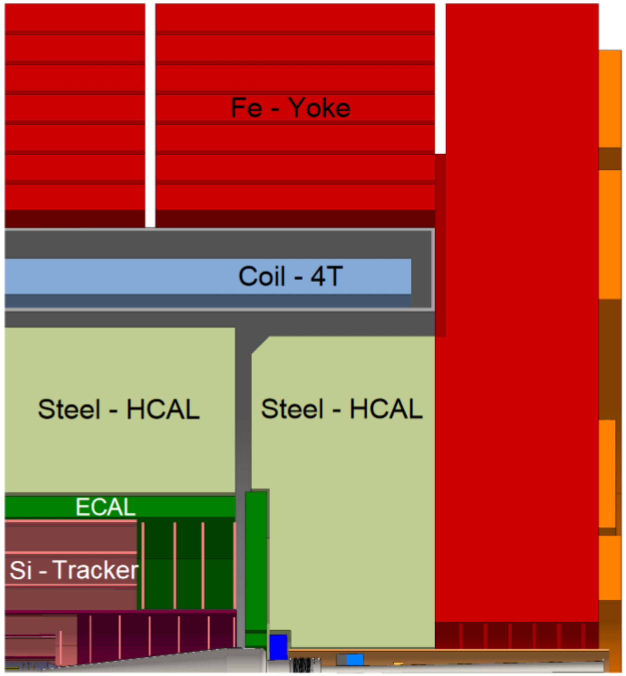

N. Alipour Tehrani et al, CLICdet: The post-CDR CLIC detector model, 2016

Higgs Physics

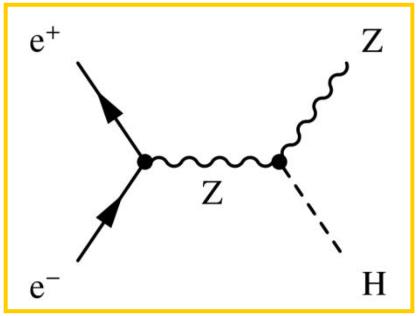

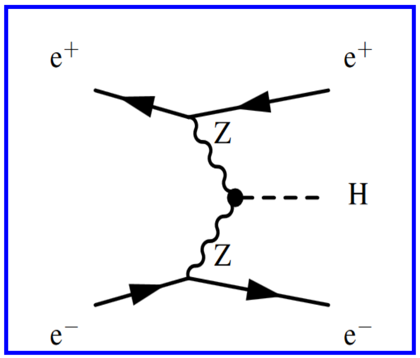

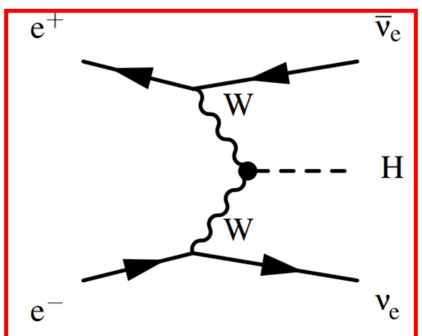

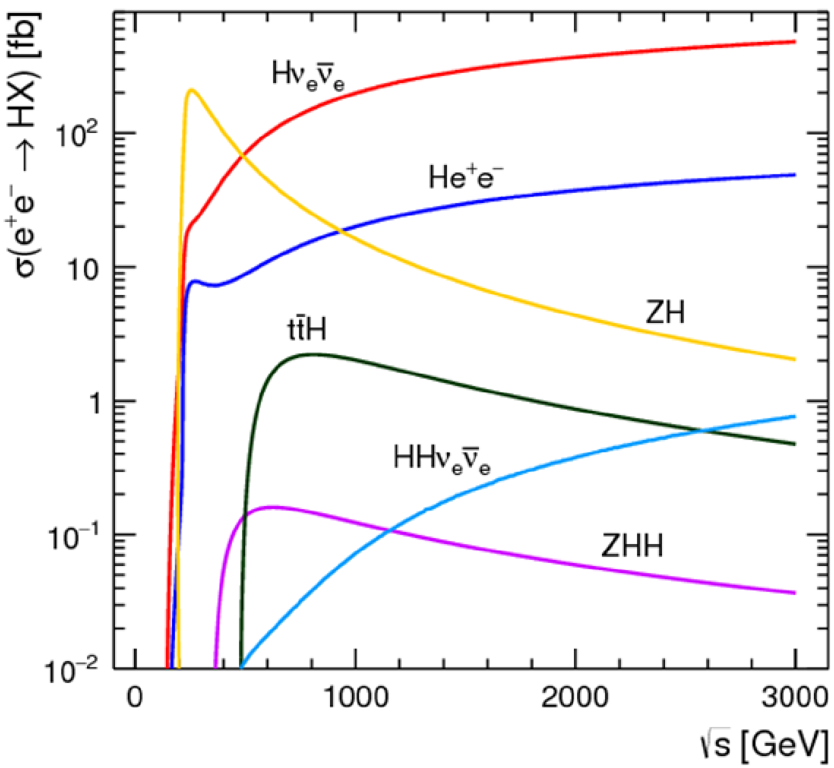

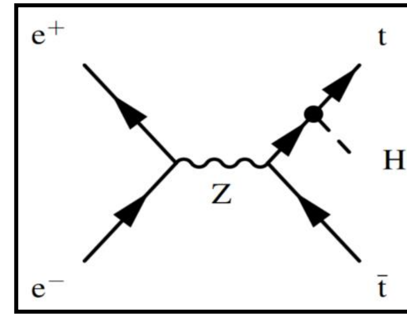

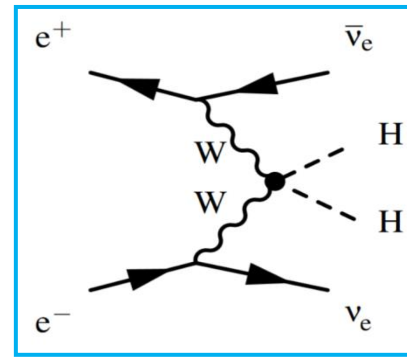

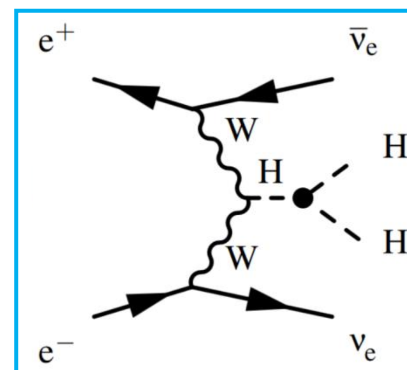

Higgsstrahlung- “The Golden Production Mode”

- Higgsstrahlung process dominates Higgs production at 380GeV
- Allows **model independent** measurements of Higgs Boson properties
- Presence of the Higgs determined purely from the properties of the recoiling Z
- Very clean signal from Z→ll:

$$\Delta \mathbf{M_H} = \mathbf{110MeV}$$

- High Statistics from Z→qq:

$$\mathbf{BR(H \rightarrow invis.) < 0.97\%\ at\ 90\%\ C.L.}$$

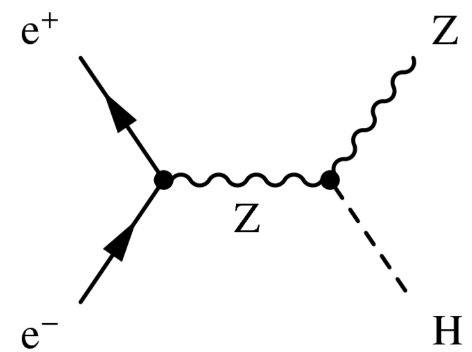

$$m_{rec}^2 = s + m_Z^2 - 2E_Z^2$$

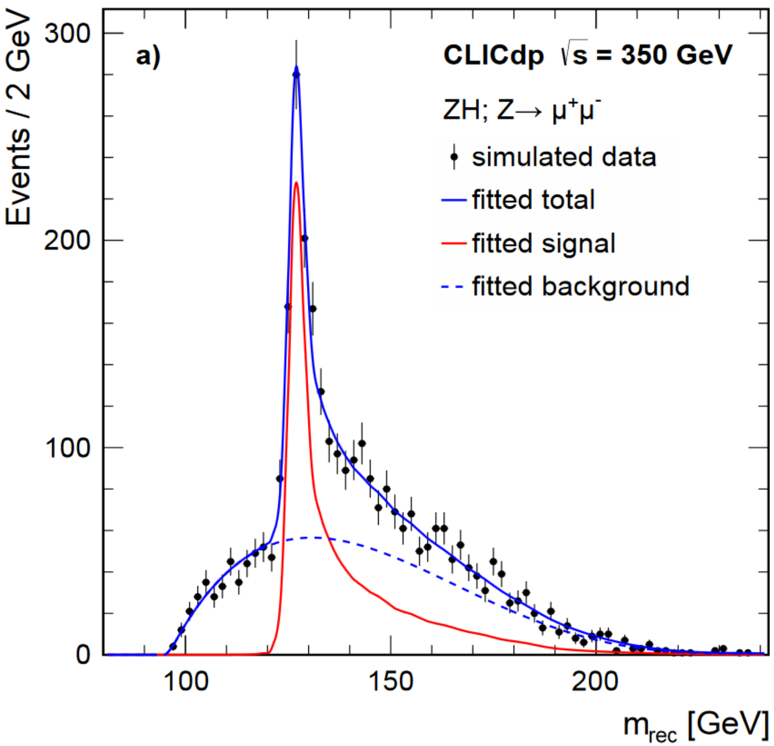

Higgs Total Width

- Calculable through ratio of four measurements:

$$Y_1 = \sigma_{ZH} = g_{HZZ}^2$$

$$Y_2 = \sigma_{ZH} \times Br(H \to b\bar{b}) = \frac{g_{HZZ}^2 g_{Hbb}^2}{\Gamma_H}$$

$$Y_3 = \sigma_{ZH} \times Br(H \to WW^*) = \frac{g_{HZZ}^2 g_{HWW}^2}{\Gamma_H}$$

$$Y_4 = \sigma_{\nu\bar{\nu}H} \times Br(H \to b\bar{b}) = \frac{g_{HWW}^2 g_{Hbb}^2}{\Gamma_H}$$

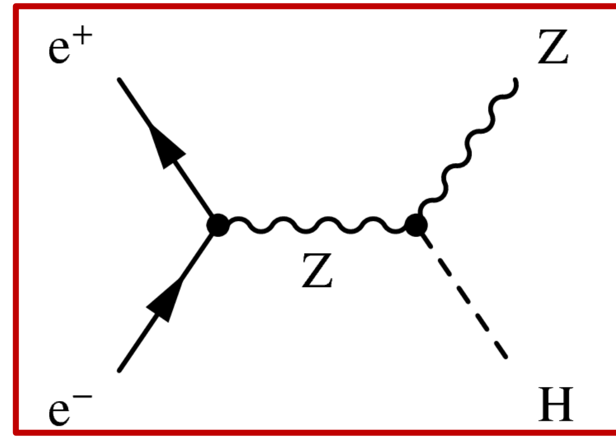

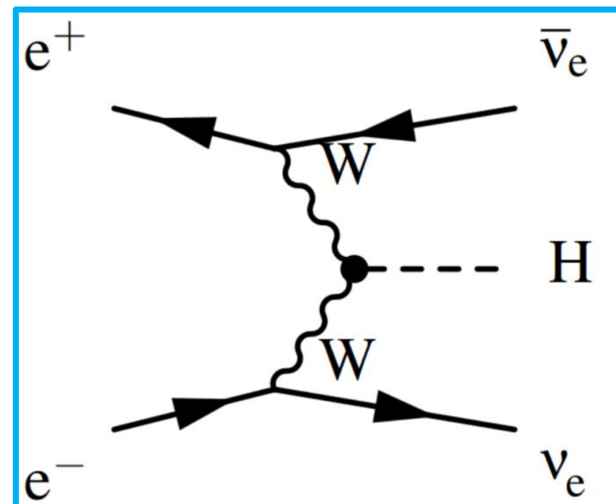

- Then:

$$\Gamma_H = \frac{Y_1^2 Y_4}{Y_2 Y_3}$$

C. Durig et al, Model Independent Determination of *HWW* coupling and Higgs total width at ILC, arxiv:1403.7734

Higgs Total Width

Channel	Measurement	Observable	Statistical precision 350 GeV 500 fb^{-1}
ZH	Recoil mass distribution	m_H	110 MeV
ZH	$\sigma(ZH) \times BR(H \to \text{invisible})$	Γ_{inv}	0.6 %
ZH	$\sigma(ZH) \times BR(Z \to l^+l^-)$	g^2_{HZZ}	3.8 %
ZH	$\sigma(ZH) \times BR(Z \to q\bar{q})$	g^2_{HZZ}	1.8 %
ZH	$\sigma(ZH) \times BR(H \to b\bar{b})$	$g^2_{HZZ} g^2_{Hbb} / \Gamma_H$	0.84 %
ZH	$\sigma(ZH) \times BR(H \to c\bar{c})$	$g^2_{HZZ} g^2_{Hcc} / \Gamma_H$	10.3 %
ZH	$\sigma(ZH) \times BR(H \to gg)$		4.5 %
ZH	$\sigma(ZH) \times BR(H \to \tau^+\tau^-)$	$g^2_{HZZ} g^2_{H\tau\tau} / \Gamma_H$	6.2 %
ZH	$\sigma(ZH) \times BR(H \to WW^*)$	$g^2_{HZZ} g^2_{HWW} / \Gamma_H$	5.1 %
$H\nu_e\bar{\nu}_e$	$\sigma(H\nu_e\bar{\nu}_e) \times BR(H \to b\bar{b})$	$g^2_{HWW} g^2_{Hbb} / \Gamma_H$	1.9 %
$H\nu_e\bar{\nu}_e$	$\sigma(H\nu_e\bar{\nu}_e) \times BR(H \to c\bar{c})$	$g^2_{HWW} g^2_{Hcc} / \Gamma_H$	14.3 %
$H\nu_e\bar{\nu}_e$	$\sigma(H\nu_e\bar{\nu}_e) \times BR(H \to gg)$		5.7 %

Combined fit:

$$\Delta(\Gamma_H) = 6.4\%$$

Higgs Couplings- Model Independent

- Direct measurement of Higgs decays allows extraction of individual couplings
- Model independent determination of couplings relies on measurement of σ(ZH) at 380GeV
  - Precision of all couplings limited by $\Delta g_{HZZ} = 0.8\%$

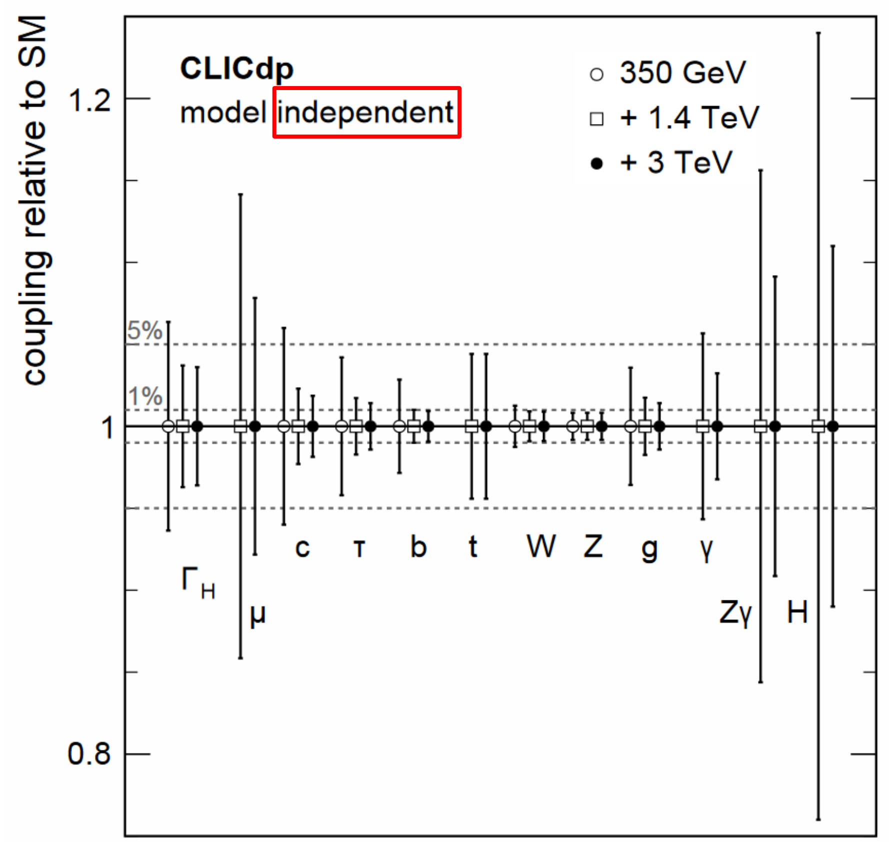

Higgs Couplings- Model Dependent

- Direct measurement of Higgs decays allows extraction of individual couplings
- Model independent determination of couplings relies on measurement of σ(ZH) at 380GeV
  - Precision of all couplings limited by $\Delta g_{HZZ} = 0.8\%$

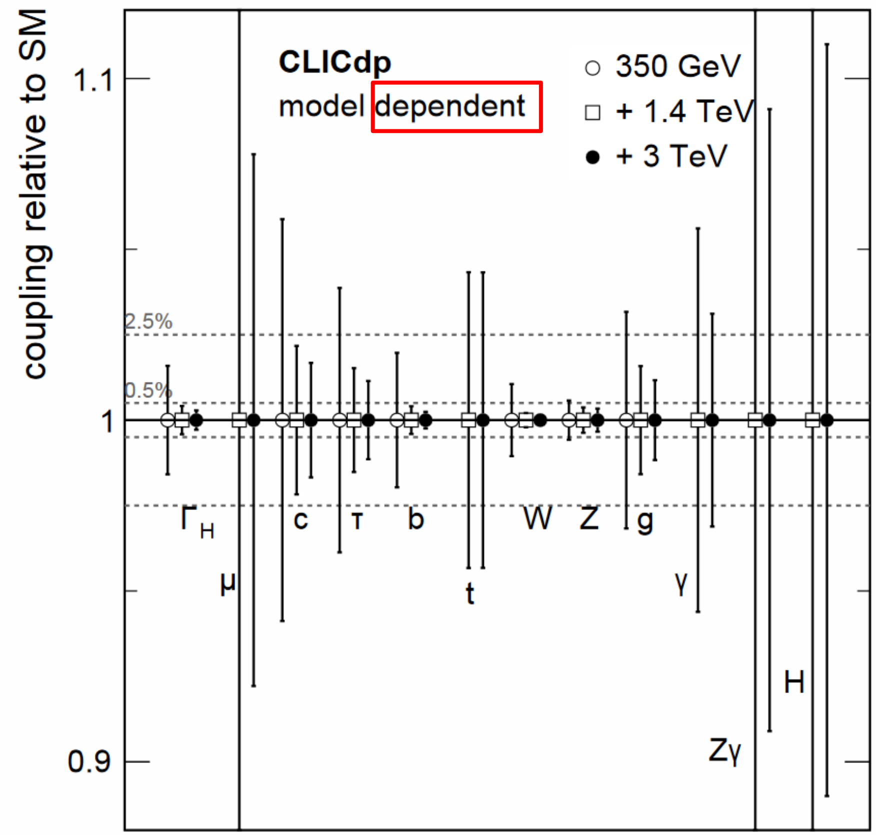

Top Physics

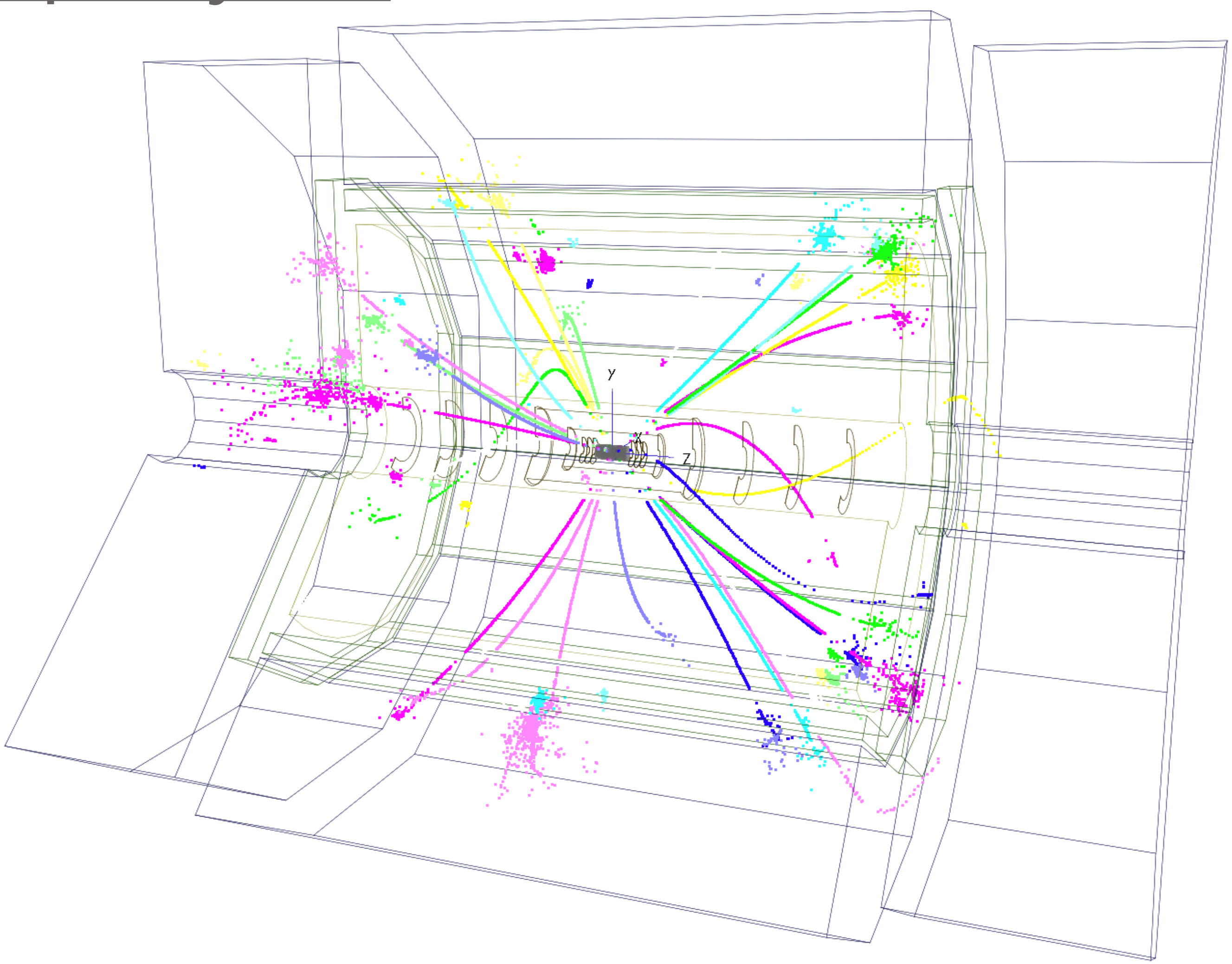

Example $t\bar{t} \rightarrow qqqqqq$ event at $\sqrt{s} = 380GeV$

Top Threshold Scan

- Top pair production cross section around the $t\bar{t}$ threshold
- Resonant-like structure → sensitive to M_t and α_s
- Mass well defined by the theory
- Perform scan around 350GeV:
  - 10 measurements, 10 fb^{-1} each

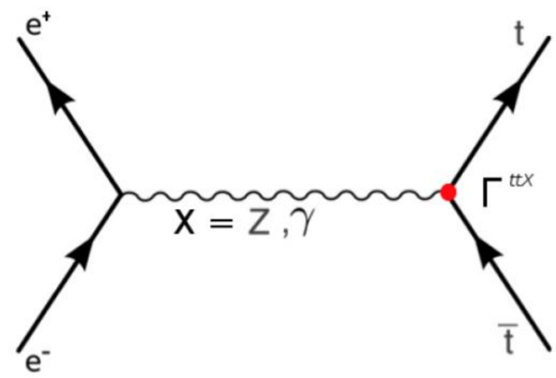

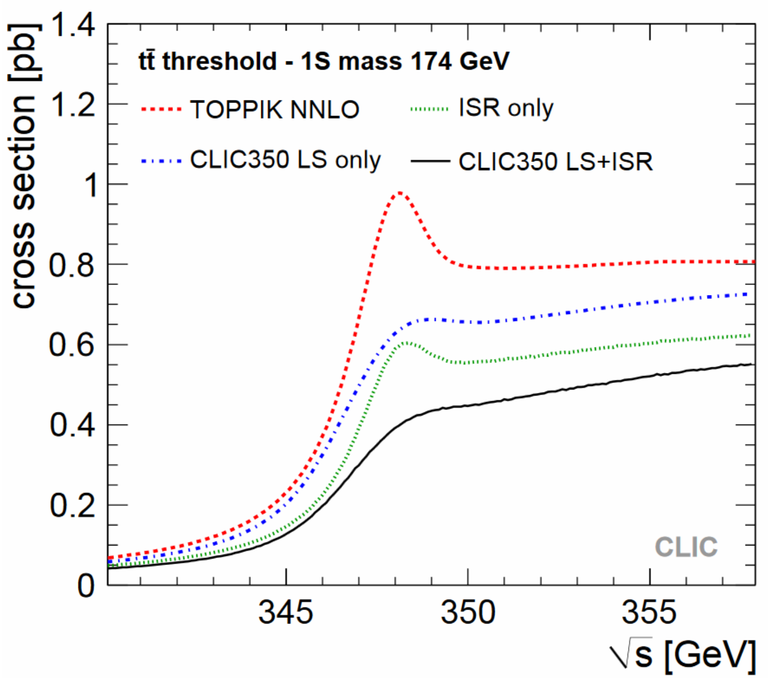

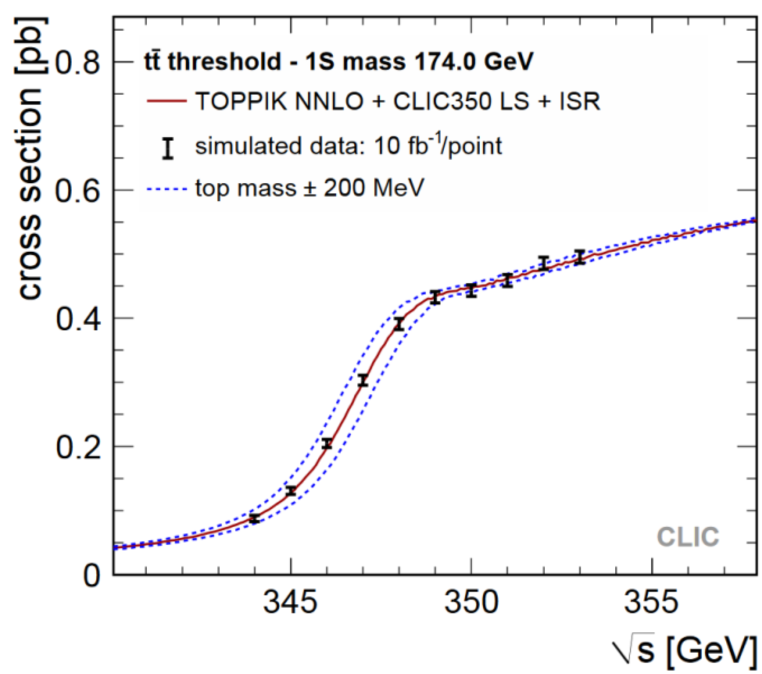

K.Seidel et al., Eur. Phys. J. C73 (2013) 2530

Top Threshold Scan

Statistical Uncertainties:

- Δ M_t: 33 MeV
- Δ Γ_t: ~ 40 MeV

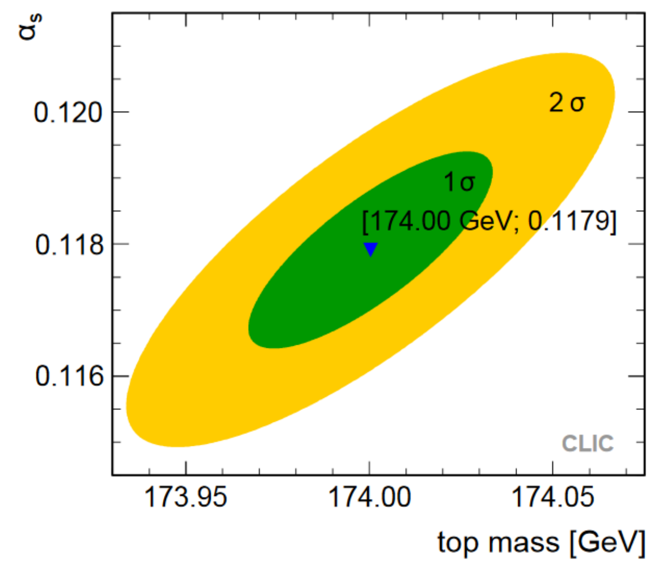

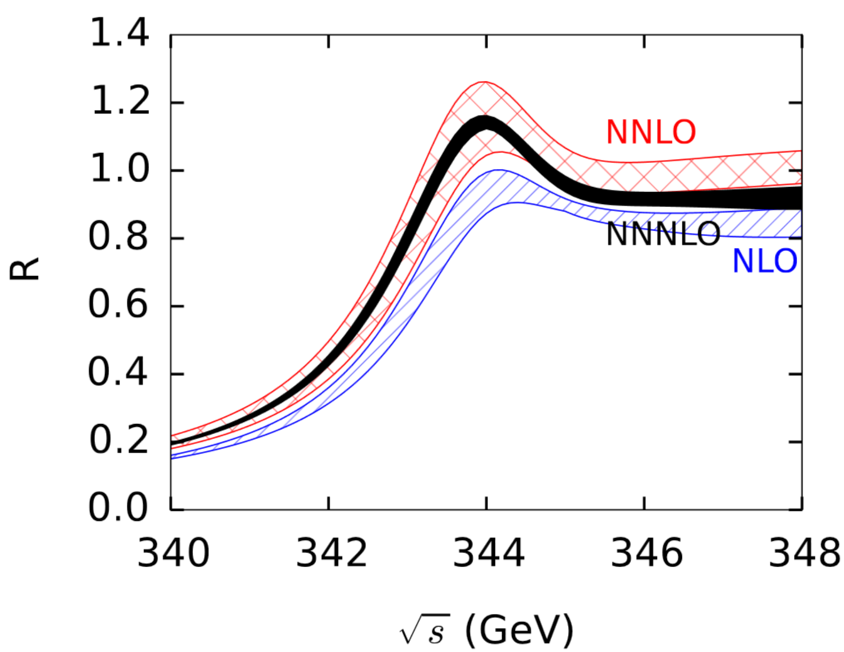

Systematic Mass Uncertainties:

- Theoretical predictions (NNNLO): ~40 MeV
- Parametric α_s uncertainty: ~30 MeV (for today's world average)
- Other uncertainties (backgrounds, spectra, etc.): on 10–20 MeV level

⇒ **total uncertainty on the top mass of ~ 50 MeV feasible**

Bottom: M.Beneke et al.,Phys. Rev. Lett. 115, 192001 (2015)

Electroweak Couplings- CP Violation

- Pair production: direct access to top electroweak couplings
- Possible higher order corrections → sensitive to BSM effects
- Couplings can be constrained through measurement of:
  - total cross-section
  - forward-backward asymmetry
  - helicity angle in top decays
- Two beam polarizations used, $P(e^-)=\pm 80\%$

$$\Gamma_{\mu}^{t\bar{t}X}(k^2,q,\bar{q}) = ie\left\{\gamma_\mu\left(\underline{F_{1V}^X}(k^2) + \gamma_5 \underline{F_{1A}^X}(k^2)\right) - \frac{\sigma_{\mu v}}{2m_t}(q+\bar{q})^v\left(i\underline{F_{2V}^X}(k^2) + \gamma_5 \underline{F_{2A}^X}(k^2)\right)\right\}$$

Electroweak Couplings- CP Violation

CP conserving couplings

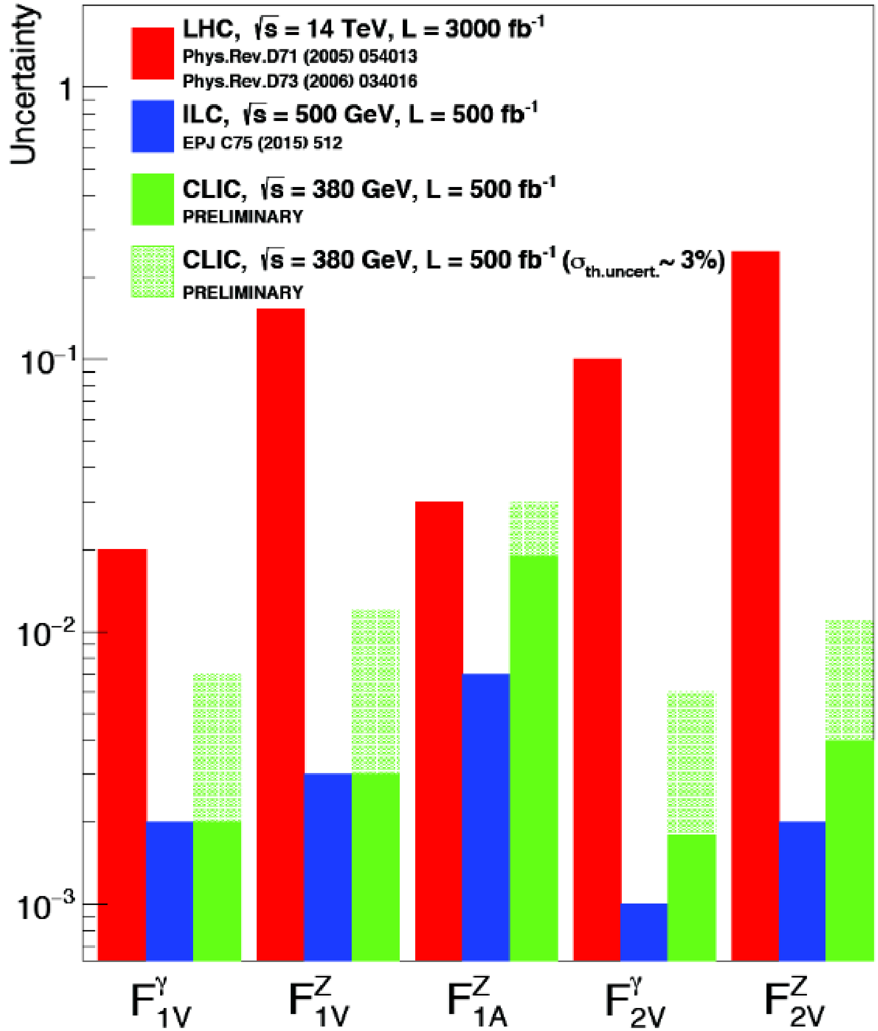

CP violating couplings

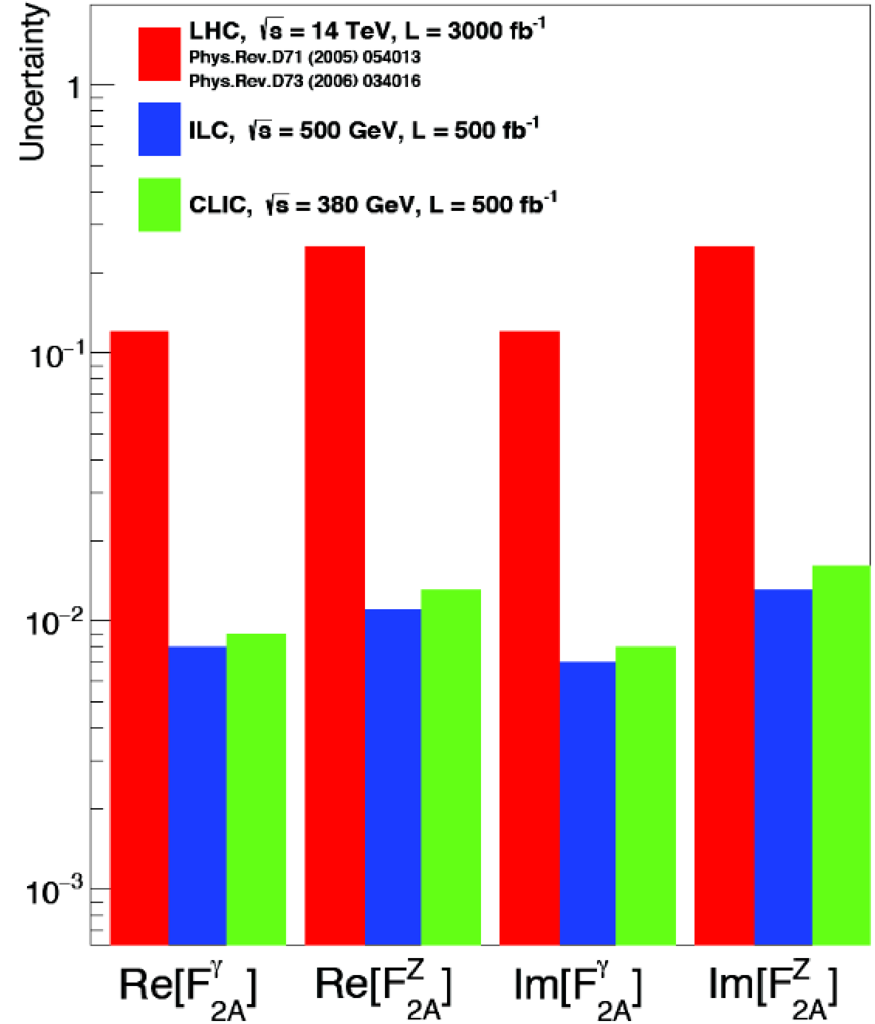

Rare Decays- FCNC

- Highly suppressed in the Standard Model:

$$BR(t \to cH) \sim 3 \times 10^{-15},\ BR(t \to c\gamma) \sim 5 \times 10^{-14}$$

- However, significant enhancement possible through many BSM effects
  - $BR(t \to cH) \sim 10^{-5}\text{-}10^{-2}$, $BR(t \to c\gamma) \sim 10^{-7}\text{-}10^{-5}$

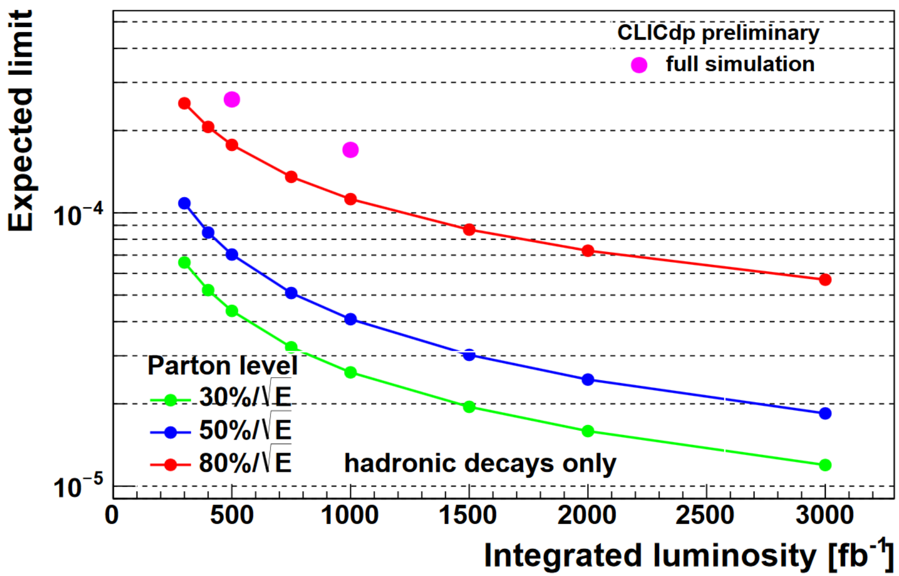

For 500fb^{-1} at 380GeV, expected limit on

$$Br(t \to ch) \times BR(h \to b\bar{b}) < 2.6 \times 10^{-4}$$

at 95 % C.L.

A.F. Zarnecki, Sensitivity of CLIC at 380 GeV to the top FCNC decay, CLICdp-CONF-2017-004

Summary

- CLIC is a multi-TeV lepton collider proposed as a future project for CERN
- The low energy run provide an ideal environment for measurement of the Higgs boson and top quark properties
- At 380GeV, Higgsstrahlung uniquely allows **model independent** precision measurements of the total Higgs width, mass and couplings. For 500fb^{-1} data:
  - $\boldsymbol{\Delta(\Gamma_H) = 6.4\%}$
  - $\boldsymbol{\Delta M_H = 110\text{MeV}}$
  - **Couplings <5%**
- A scan of the $t\bar{t}$ production threshold will allow measurement of the top mass, $\boldsymbol{\Delta M_t \sim 50\text{MeV}}$
- Measurement of $t\bar{t}$ production at 380GeV → unprecedented precision on electroweak form factors

Backup

Higgs Results for Higher Energies

Channel	Measurement	Observable	Statistical precision: 1.4 TeV $1.5\,ab^{-1}$	Statistical precision: 3 TeV $2.0\,ab^{-1}$
$H\nu_e\bar{\nu}_e$	$H \to b\bar{b}$ mass distribution	m_H	47 MeV	44 MeV
$H\nu_e\bar{\nu}_e$	$\sigma(H\nu_e\bar{\nu}_e) \times BR(H \to b\bar{b})$	$g^2_{HWW} g^2_{Hbb} / \Gamma_H$	0.4 %	0.3 %
$H\nu_e\bar{\nu}_e$	$\sigma(H\nu_e\bar{\nu}_e) \times BR(H \to c\bar{c})$	$g^2_{HWW} g^2_{Hcc} / \Gamma_H$	6.1 %	6.9 %
$H\nu_e\bar{\nu}_e$	$\sigma(H\nu_e\bar{\nu}_e) \times BR(H \to gg)$		5.0 %	4.3 %
$H\nu_e\bar{\nu}_e$	$\sigma(H\nu_e\bar{\nu}_e) \times BR(H \to \tau^+\tau^-)$	$g^2_{HWW} g^2_{H\tau\tau} / \Gamma_H$	4.2 %	4.4 %
$H\nu_e\bar{\nu}_e$	$\sigma(H\nu_e\bar{\nu}_e) \times BR(H \to \mu^+\mu^-)$	$g^2_{HWW} g^2_{H\mu\mu} / \Gamma_H$	38 %	25 %
$H\nu_e\bar{\nu}_e$	$\sigma(H\nu_e\bar{\nu}_e) \times BR(H \to \gamma\gamma)$		15 %	10 %*
$H\nu_e\bar{\nu}_e$	$\sigma(H\nu_e\bar{\nu}_e) \times BR(H \to Z\gamma)$		42 %	30 %*
$H\nu_e\bar{\nu}_e$	$\sigma(H\nu_e\bar{\nu}_e) \times BR(H \to WW^*)$	g^4_{HWW} / Γ_H	1.0 %	0.7 %*
$H\nu_e\bar{\nu}_e$	$\sigma(H\nu_e\bar{\nu}_e) \times BR(H \to ZZ^*)$	$g^2_{HWW} g^2_{HZZ} / \Gamma_H$	5.6 %	3.9 %*
He^+e^-	$\sigma(He^+e^-) \times BR(H \to b\bar{b})$	$g^2_{HZZ} g^2_{Hbb} / \Gamma_H$	1.8 %	2.3 %*
$t\bar{t}H$	$\sigma(t\bar{t}H) \times BR(H \to b\bar{b})$	$g^2_{Htt} g^2_{Hbb} / \Gamma_H$	8.4 %	–
$HH\nu_e\bar{\nu}_e$	$\sigma(HH\nu_e\bar{\nu}_e)$	λ	32 %	16 %
$HH\nu_e\bar{\nu}_e$	with −80 % e^- polarisation	λ	24 %	12 %

Table 29: Summary of the precisions obtainable for the Higgs observables in the higher-energy CLIC stages for integrated luminosities of $1.5\,ab^{-1}$ at $\sqrt{s} = 1.4\,TeV$, and $2.0\,ab^{-1}$ at $\sqrt{s} = 3\,TeV$. In both cases unpolarised beams have been assumed. The '–' indicates that a measurement is not possible or relevant at this centre-of-mass energy. Numbers marked with $*$ were extrapolated from $\sqrt{s} = 1.4\,TeV$ to $\sqrt{s} = 3\,TeV$ as explained in the text. For the branching ratios, the measurement precision refers to the expected statistical uncertainty on the product of the relevant cross section and branching ratio; this is equivalent to the expected statistical uncertainty of the product of couplings divided by Γ_H, as indicated in the third column. For the measurements from the $HH\nu_e\bar{\nu}_e$ process, the measurement precisions give the expected statistical uncertainties on the self-coupling parameter λ.

Higgs Results for Higher Energies

Model Independent Results

Parameter	Relative precision		
	350 GeV 500 fb^{-1}	+ 1.4 TeV + 1.5 ab^{-1}	+ 3 TeV + 2 ab^{-1}
g_{HZZ}	0.8 %	0.8 %	0.8 %
g_{HWW}	1.3 %	0.9 %	0.9 %
g_{Hbb}	2.8 %	1.0 %	0.9 %
g_{Hcc}	6.0 %	2.3 %	1.9 %
$g_{H\tau\tau}$	4.2 %	1.7 %	1.4 %
$g_{H\mu\mu}$	–	14.1 %	7.8 %
g_{Htt}	–	4.4 %	4.4 %
$g^{\dagger}_{Hgg}$	3.6 %	1.7 %	1.4 %
$g^{\dagger}_{H\gamma\gamma}$	–	5.7 %	3.2 %
$g^{\dagger}_{HZ\gamma}$	–	15.6 %	9.1 %
Γ_H	6.4 %	3.7 %	3.6 %

Model Dependent Results

Parameter	Relative precision		
	350 GeV 500 fb^{-1}	+ 1.4 TeV + 1.5 ab^{-1}	+ 3 TeV + 2 ab^{-1}
κ_{HZZ}	0.57 %	0.37 %	0.34 %
κ_{HWW}	1.1 %	0.21 %	0.14 %
κ_{Hbb}	2.0 %	0.41 %	0.24 %
κ_{Hcc}	5.9 %	2.2 %	1.7 %
$\kappa_{H\tau\tau}$	3.9 %	1.5 %	1.1 %
$\kappa_{H\mu\mu}$	–	14.1 %	7.8 %
κ_{Htt}	–	4.3 %	4.3 %
κ_{Hgg}	3.2 %	1.6 %	1.2 %
$\kappa_{H\gamma\gamma}$	–	5.6 %	3.1 %
$\kappa_{HZ\gamma}$	–	15.6 %	9.1 %
$\Gamma_{H,md,derived}$	1.6 %	0.41 %	0.28 %

New CLIC detector parameters

Table 1: Comparison of key parameters of the different CLIC detector concepts. CLIC_ILD and CLIC_SiD values are taken from the CDR [3]. The inner radius of the electromagnetic calorimeter (ECAL) is given by the smallest distance of the calorimeter to the main detector axis. For the hadronic calorimeter (HCAL), materials are given separately for the barrel and the endcap.

Concept	CLICdet	CLIC_ILD	CLIC_SiD
Vertex inner radius [mm]	31	31	27
Tracker technology	Silicon	TPC/Silicon	Silicon
Tracker half length [m]	2.2	2.3	1.5
Tracker outer radius [m]	1.5	1.8	1.3
ECAL absorber	W	W	W
ECAL X_0	22	23	23
ECAL barrel r_{min} [m]	1.5	1.8	1.3
ECAL barrel Δr [mm]	202	172	139
ECAL endcap z_{min} [m]	2.31	2.45	1.66
ECAL endcap Δz [mm]	202	172	139
HCAL absorber barrel / endcap	Fe / Fe	W / Fe	W / Fe
HCAL λ_I	7.5	7.5	7.5
HCAL barrel r_{min} [m]	1.74	2.06	1.45
HCAL barrel Δr [mm]	1590	1238	1177
HCAL endcap z_{min} [m]	2.45	2.65	1.80
HCAL endcap Δz [mm]	1590	1590	1595
Solenoid field [T]	4	4	5
Solenoid bore radius [m]	3.5	3.4	2.7
Solenoid length [m]	8.3	8.3	6.5
Overall height [m]	12.9	14.0	14.0
Overall length [m]	11.4	12.8	12.8
Overall weight [t]	8100	10800	12500

Energy Staging Parameters

Table 9: Parameters for the CLIC energy stages. The power consumptions for the 1.5 and 3 TeV stages are from the CDR; depending on the details of the upgrade they can change at the percent level.

Parameter	**Symbol**	**Unit**	**Stage 1**	**Stage 2**	**Stage 3**
Centre-of-mass energy	$\sqrt{s}$	GeV	380	1500	3000
Repetition frequency	f_{rep}	Hz	50	50	50
Number of bunches per train	n_b		352	312	312
Bunch separation	Δt	ns	0.5	0.5	0.5
Pulse length	τ_{RF}	ns	244	244	244
Accelerating gradient	G	MV/m	72	72/100	72/100
Total luminosity	$\mathscr{L}$	$10^{34}\ \mathrm{cm^{-2}s^{-1}}$	1.5	3.7	5.9
Luminosity above 99% of $\sqrt{s}$	$\mathscr{L}_{0.01}$	$10^{34}\ \mathrm{cm^{-2}s^{-1}}$	0.9	1.4	2
Main tunnel length		km	11.4	29.0	50.1
Number of particles per bunch	N	10^9	5.2	3.7	3.7
Bunch length	σ_z	μm	70	44	44
IP beam size	σ_x/σ_y	nm	149/2.9	$\sim$ 60/1.5	$\sim$ 40/1
Normalised emittance (end of linac)	$\varepsilon_x/\varepsilon_y$	nm	920/20	660/20	660/20
Normalised emittance (at IP)	$\varepsilon_x/\varepsilon_y$	nm	950/30	—	—
Estimated power consumption	P_{wall}	MW	252	364	589

Higgs Couplings- Model Dependent

- Direct measurement of Higgs decays allows extraction of individual couplings
- Model independent determination of couplings relies on measurement of σ(ZH) at 380GeV
  - Precision of all couplings limited by $\Delta g_{HZZ} = 0.8\%$

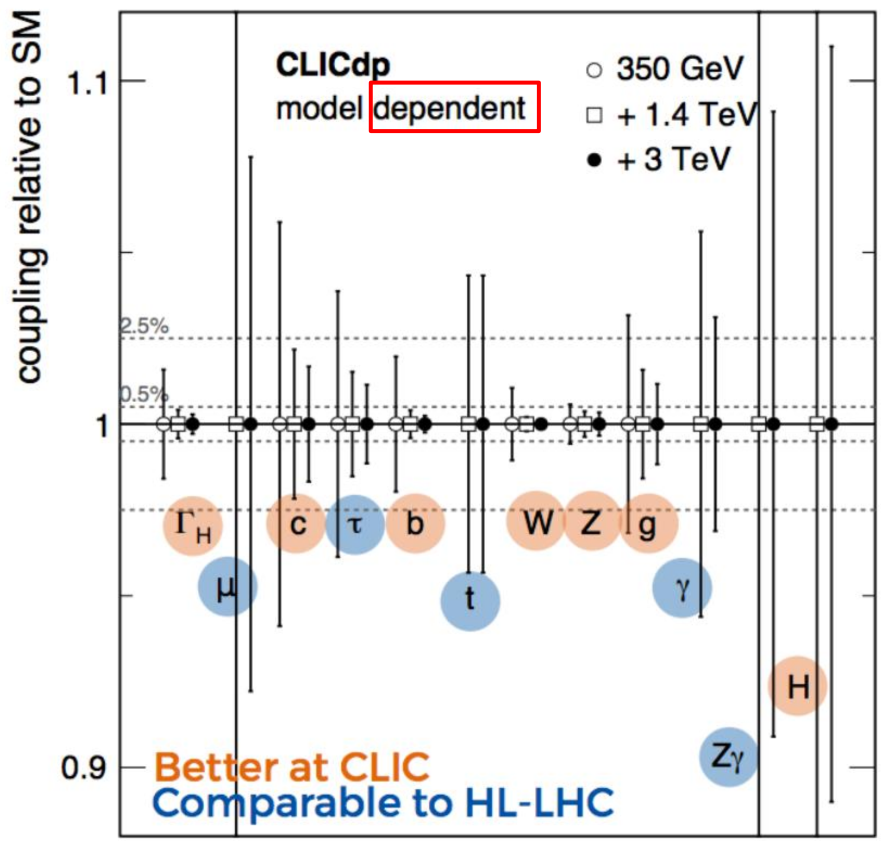

Accelerator design for 3TeV

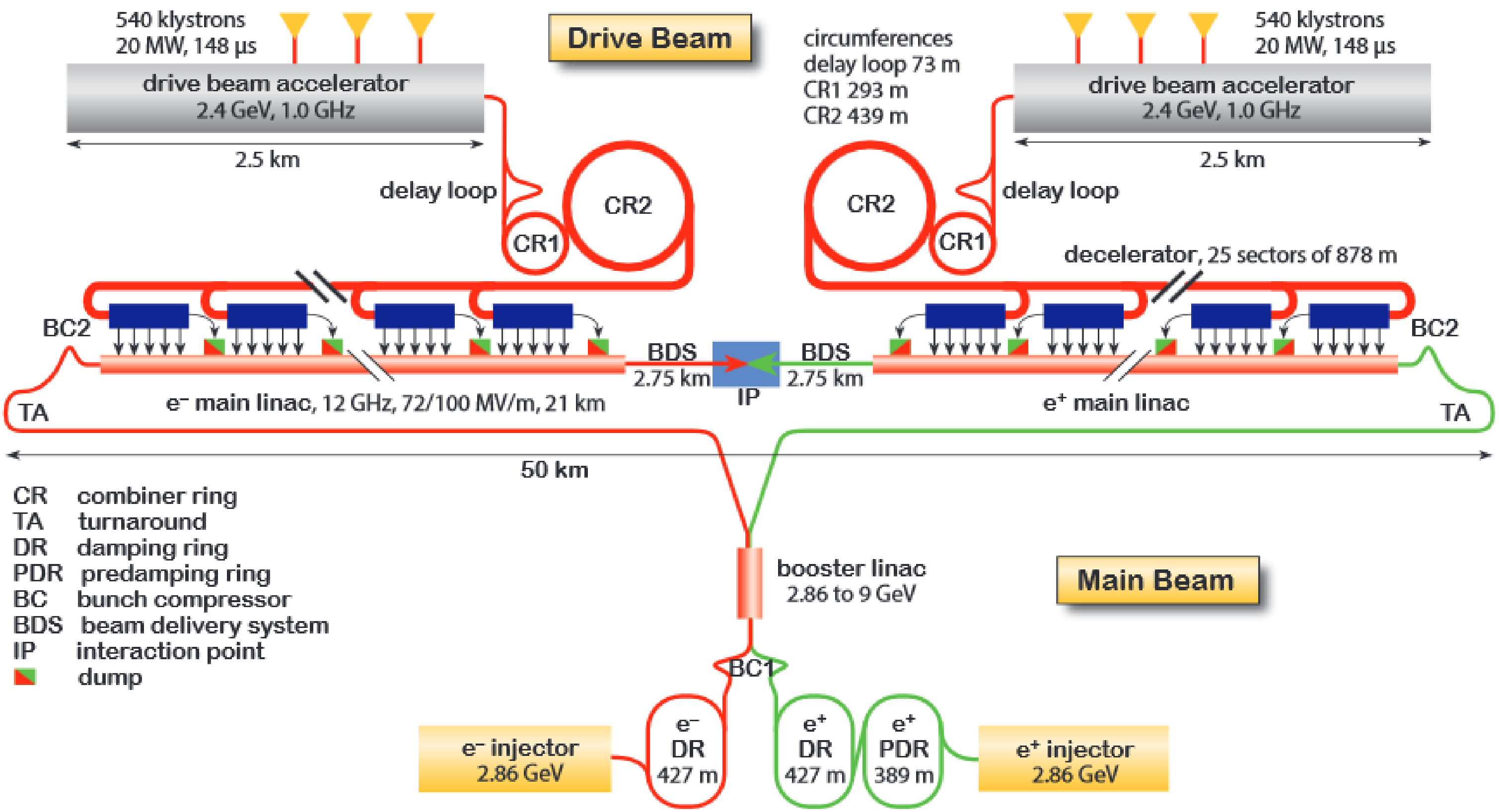

Figure 19: Overview of the CLIC layout at $\sqrt{s} = 3$ TeV.